Mechanism of Clay Tactoid Exfoliation in Epoxy−Clay Nanocomposites

Tie Lan, Padmananda D. Kaviratna, and Thomas J. Pinnavaia*

Department of Chemistry and Center for Fundamental Materials Research, Michigan State University, East Lansing, Michigan 48824

Received May 23, 1995. Revised Manuscript Received August 16, 1995®

Monolithic epoxy exfoliated-clay nanocomposites have been prepared by the reaction of alkylammonium-exchanged smectite clays with diglycidyl ether of bisphenol A and *m*-phenylenediamine as the curing agent. Exfoliation of the clay tactoids in the polymer matrix is dependent on the accessibility of the epoxy and diamine monomers to the clay galleries and the relative rates of intra- and extragallery network formation. Initial epoxy access to the gallery surfaces is provided by solvation interactions with the alkyl chains on the onium ions. Regardless of the clay layer charge density, the onium ions adopt a vertical orientation in the galleries in order to optimize interactions with the epoxide resin. Under amine curing conditions where the intra- and extragallery polymerization rates are comparable, the clay tactoids are exfoliated into segregated 10-Å-thick layers. Exfoliation is facilitated by acidic exchange cations that can catalyze the intragallery epoxide polymerization process. Nonacidic quaternary ammonium ions tend to form intercalated rather than exfoliated clay nanocomposites. Access to the gallery region of the clay under polymerization conditions is determined by the population density of the gallery onium ions. In general, low charge density clays (hectorite and montmorillonite) are more readily accessible for intragallery polymerization than high charge density analogues (fluorohectorite and vermiculite). Thus, low charge density clays typically provide nanocomposites with a high degree of layer exfoliation, as judged by XRD. Preliminary mechanical measurements show that exfoliated epoxy−clay nanocomposites have higher moduli than intercalated clay composites.

Introduction

The properties of the hybrid organic−inorganic composite materials are greatly influenced by the length scale of component phases.[1-4] Nanoscale dispersion of the inorganic component typically optimizes the mechanical properties of the composite. One successful approach to enhancing inorganic particle dispersion is the in situ polymerization of metal alkoxides in organic polymer matrices via the sol−gel process. In these systems the inorganic components are formed by the hydrolysis and condensation of mononuclear precursors, such as tetraethoxysilane (TEOS) and tetramethoxysilane (TMOS). Nanoscale hybrid organic−inorganic composites containing silica have been reported for many polymer systems, including polydimethysiloxane,[5] poly(tetramethylene oxide),[6] polymethacrylate,[7] epoxides,[8] and polyimides.[9,10] Although novel approaches to nonshrinkable hybrids have been recently reported,[11] it is generally difficult to control sample shrinkage owing to the loss of volatile byproducts formed in the hydrolysis/condensation reactions associated with the sol−gel process.

Inorganic materials that can be broken down into their nanoscale building blocks are good alternatives to the sol−gel process for the preparation of hybrid organic−inorganic composites. For instance, the exfoliation of the 10-Å-thick layers of smectite clays in polymer matrices is one such promising route to nanocomposite formation.[2] Ion exchange of the Na^+ or Ca^{2+} gallery cations in the pristine mineral by inorganic, organic, and complex cations allows modification of the gallery surfaces for intercalation of organic polymer precursors. Also, the high aspect ratios of the exfoliated clay layers, typically in the range 200−2000, afford reinforcement properties comparable to fibers for certain polymer matrices.

In general, the dispersion of clay particles in a polymer matrix can result in the formation of three general types of composite materials.[12] These are illustrated in Figure 1. Conventional composites contain clay tactoids with the layers aggregated in unintercalated face−face form. In this case the clay tactoids are simply dispersed as a segregated phase. Intercalated clay composites are intercalation compounds of definite structure formed by the insertion of one or more molecular layers of polymer into the clay host galleries. The clay content of the intercalates is typically high (>50%), and the properties usually resemble those of the ceramic host. In contrast, exfoliated polymer−clay

---

® Abstract published in *Advance ACS Abstracts,* September 15, 1995.

(1) Whitesides, G. M.; Mathias, T. P.; Seto, C. T. *Science* **1991,** *254,* 1312.

(2) Giannelis, E. P. *JOM* **1992,** *44,* 28.

(3) Gleiter, H. *Adv. Mater.* **1992,** *4,* 474.

(4) Novak, B. *Adv. Mater.* **1993,** *5,* 422.

(5) Langley, N. R.; Mbah, G. C.; Freeman, H. A.; Huang, H.; Siochi, E. J.; Ward, T. C.; Wilkes, G. *J. Colloid Interface Sci.* **1991,** *143,* 309.

(6) Glaser, R. H.; Wilkes, G. *Polym. Bull.* **1989,** *19,* 51.

(7) Philipp, G.; Schimdt, H. *J. Non-Cryst. Solids* **1984,** 283.

(8) Philipp, G.; Schimdt, H. *J. Non-Cryst. Solids.* **1986,** *82,* 31.

(9) Wang, S.; Ahmad, Z.; Mark, J. E. *Proc. ACS, Div. Polym. Mater.: Sci. Eng. (PMSE)* **1994,** *70,* 305.

(10) Kakimoto, M.; Iyoku, Y.; Morikawa, A.; Yamaguchi, H.; Imai, Y. *Polym. Prepr.* **1994,** *35-1,* 393.

(11) Ellsworth, M. W.; Novak, B. M. *Chem. Mater.* **1993,** *5,* 839.

(12) Lan, T.; Pinnavaia, T. J., *Chem. Mater.* **1994,** *6,* 2216.

0897-4756/95/2807-2144$09.00/0

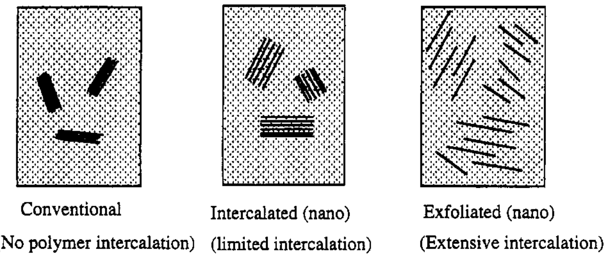

Figure 1. Schematic illustrations of the three possible types of polymer−clay composites.

nanocomposites have a low clay content, a monolithic structure, a separation between layers that depends on the polymer content of the composite, and properties that reflect those of the nanoconfined polymer.

Intercalated polymer−clay nanocomposites have been synthesized by direct polymer intercalation[13,14] and in situ intercalative polymerization of monomers in the clay galleries.[15−17] Owing to the spatial confinement of the polymer between the dense clay layers, intercalated polymer−clay nanocomposites can exhibit impressive conductivity properties[18] and barrier properties.[19] However, it is relatively difficult to achieve complete exfoliation of smectite clays into a continuous polymer matrix, because of the strong electrostatic attraction between the silicate layers and the intergallery cations. The first hybrid polymer−clay composite with an exfoliated clay structure was the nylon-6-montmorillonite hybrid reported by Toyota researchers.[20,21] This hybrid material exhibited greatly improved mechanical properties and thermal stability.[22−24] Also, exfoliated polyether−clay nanocomposites have been prepared by the homopolymerization of an epoxy resin in the galleries of acidic alkylammonium ion exchanged forms of montmorillonite.[25−27] However, due to their powdery texture, the polyether−clay nanocomposites were not suitable for mechanical measurements.

Recently, exfoliated layered silicate−epoxy nanocomposites have been prepared from the diglycidyl ether of bisphenol-A and nadic methyl anhydride.[28] The dynamic storage modulus of the nanocomposite containing 4 vol % silicate was approximately 58% higher in the glassy region and 450% higher in the rubbery plateau region compared to the pristine polymer. Concurrently, we found that monolithic exfoliated clay nanocomposites can be formed by preswelling alkylammonium ion exchanged forms of the clays with epoxy resin prior to curing.[12,29] Dramatic improvement in the tensile strength and modulus was realized, particularly when the matrix exhibited a subambient glass transition temperature. For instance, the reinforcement provided by the silicate layers at 16 wt % loading was manifested by a more than 10-fold improvements in both tensile strength and modulus.

In view of the importance of clay exfoliation in improving the mechanical properties of epoxies, we investigate in the present work the mechanism of smectite clay swelling by the epoxy resin, and the subsequent formation of an exfoliated clay nanocomposite upon curing with *m*-phenylenediamine.

Experimental Section

Materials. Sodium hectorite from California, montmorillonite from Wyoming and vermiculite from Texas were obtained from the Source Clay Minerals Repository at the University of Missouri−Columbia. Synthetic fluorohectorite and laponite were obtained from Corning, Inc., and Laporte Co., respectively. The cation exchange capacity (CEC) value, as determined by the displacement of ammonia from ammonium-saturated samples using NaOH and ammonia specific electrode, was 67, 90, 122, and 200 mequiv/100 g for hectorite, montmorillonite, fluorohectorite, and vermiculite respectively. Epoxy resin Epon-828, the diglycidyl ether of bisphenol A with a molecular weight of 380, was obtained from Shell Co:

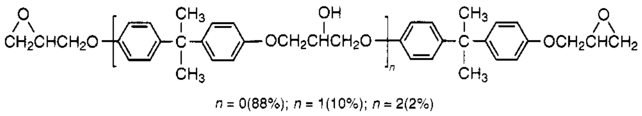

m-Phenylenediamine (mPDA) was used as a curing agent for the epoxy resin:

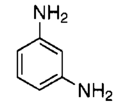

Alkylammonium salt solutions were prepared by the addition of 1 equiv of 0.05 M HCl to a solution of the corresponding amine. All the other chemicals used in this work were purchased from Aldrich Chemical Co. and used without further purification.

Ion Exchanged Clays. Na^+ and NH_4^+ exchanged clays were obtained by reaction of NaCl or NH_4Cl (1.0 M, 500 mL) with the pristine clay (2.0 g) at 75 °C for 24 h. The exchanged clays were washed with distilled water until no chloride was detected with 0.1 N $AgNO_3$ solution and then air dried. Alkylammonium exchanged clays were prepared by previously described methods.[30] A 500-mL quantity of 0.05 M alkylammonium chloride/bromide in ethanol:water (1:1) solution and 2 g of clay was heated at 75 °C for 24 h. The exchanged clays were washed with 1:1 ethanol:water mixture several times until no chloride was detected with 0.1 N $AgNO_3$ solution and air dried. The clays were ground with a mortar and pestle, and the 50−60 μm fraction was collected.

Preparation of Epoxy−Clay Composites. Epoxy−clay mixtures were obtained by mixing the desired amount of clay

---

(13) Theng, B. K. G. *Formation and Properties of Clay-Polymer Complexes*; Elsevier: New York, 1979.

(14) Vaia, R. A.; Ishii, H.; Giannelis, E. P. *Chem. Mater.* **1993**, *5*, 1694.

(15) Kato, C.; Kuroda, K.; Misawa, M. *Clays Clay Miner.* **1979**, *27*, 129.

(16) Sugahara, Y.; Sugiyama, T.; Nagayama, T.; Kuroda, K.; Kato, C. *J. Ceram. Soc. Jpn.* **1992**, *100*, 413.

(17) Messersmith, P. B.; Giannelis, E. P. *Chem. Mater.* **1993**, *5*, 1064.

(18) Mehrotra, Giannelis, E. P. *Solid State Commun.* **1991**, *77*, 155.

(19) Lan, T.; Kaviratna, P. D.; Pinnavaia, T. J. *Chem. Mater.* **1994**, *6*, 573.

(20) Fukushima, Y.; Inagaki, S. *J. Inclusion Phenom.* **1987**, *5*, 473.

(21) Fukushima, Y.; Okada, A.; Kawasumi, M.; Kurauchi, T.; Kamigaito, O. *Clay Miner.* **1988**, *23*, 27.

(22) Usuki, A.; Kawasumi, M.; Kojima, Y.; Okada, A.; Kurauchi, T.; Kamingato, O. *J. Mater. Res.* **1993**, *8*, 1174.

(23) Usuki, A.; Kojima, Y.; Kawasumi, M.; Okada, A.; Fukushima, Y.; Kurauchi, T.; Kamigaito, O. *J. Mater. Res.* **1993**, *8*, 1179.

(24) Kojima, Y.; Usuki, A.; Kawasumi, M.; Okada, A.; Fukushima, Y.; Kurauchi, T.; Kamigaito, O. *J. Mater. Res.* **1993**, *8*, 1185.

(25) Kaviratna, P. D.; Lan, T.; Pinnavaia, T. J. *Polym. Prepr.* **1994**, *35-1*, 788.

(26) Pinnavaia, T. J.; Lan, T.; Kaviratna, P. D.; Wang, M. Clay-Polymer Nanocomposites: Polyether and Polyimide Systems. *MRS Symp., Paper* **1994**, N-2.8.

(27) Wang, M.; Pinnavaia, T. J. *Chem. Mater.* **1994**, *6*, 468.

(28) Messersmith, P. B.; Giannelis, E. P. *Chem. Mater.* **1994**, *6*, 1719.

(29) Lan, T.; Kaviratna, P. D.; Pinnavaia, T. J. *Proc. ACS, Div. Polym. Mater.: Sci. Eng. (PMSE)* **1994**, *71*, 528.

(30) Lee, T. Ph.D. Thesis, Michigan State University, 1992.

(31) Schiering, D. W.; Katon, J. E.; Drzal, L. T.; Gupta, V. B. *J. Appl. Polym. Sci.* **1987**, *34*, 2367.

Table 1. Basal Spacings (d_{001}, Å) of Alkylammonium Exchanged Montmorillonites

gallery cation	initial cation orientation[a]	air-dried	epoxy solvated	calculated value[b]
$CH_3(CH_2)_3NH_3^+$	monolayer	13.5	16.5	19.6
$CH_3(CH_2)_7NH_3^+$	monolayer	13.8	27.2	24.7
$CH_3(CH_2)_9NH_3^+$	monolayer	13.8	30.0	27.2
$CH_3(CH_2)_{11}NH_3^+$	bilayer	15.6	31.9	29.8
$CH_3(CH_2)_{15}NH_3^+$	bilayer	17.6	34.1	34.9
$CH_3(CH_2)_{17}NH_3^+$	bilayer	18.0	36.7	37.4

[a] Orientation of the alkylammonium ion under air-dried conditions. [b] Basal spacings are calculated assuming the gallery cation adopts a vertical orientation relative to the layer and an all trans configuration such that $d_{001} = 12.8 + 3.0 + 1.27(n - 1)$ (Å), where 12.8 Å is the d_{001} of NH_4^+–montmorillonite, 3.0 Å is the size of $-CH_3$ end group, and 1.27 Å is the distance increase upon adding one $-CH_2-$ group to the alkyl chain.[32]

with the epoxy resin at 75 °C and adding 1 equiv of mPDA (14.5 wt % of the Epon-828 content). The mixtures were degassed in a vacuum oven (~25 Torr) for a short period of time. Samples for mechanical testing were transferred into a silicone rubber mold for curing at 75 °C for 2 h, followed by an additional 2 h cure at 125 °C.

XRD and TEM. X-ray powder diffraction patterns were obtained by using a Rigaku X-ray diffractometer equipped with Cu Kα radiation and a curved graphite crystal monochromator. Samples of epoxy-solvated clays were prepared by applying the epoxy–clay mixture as a thin film on glass slides. Composite samples for X-ray diffraction and TEM analyses were prepared by crushing the specimens and collecting the particles in the size range 150–180 μm. Samples of TEM were embedded in a capsule with an embedding agent (Hard-Spurr) polymerized at 60 °C for 48 h. The embedded sample was ultrathin-sectioned by using a microtome equipped with a glass knife. The thin sections were 600–900 Å thick. Transmission electron micrographs were obtained with a JEOL-100CX using an acceleration voltage of 100 kV.

Mechanical Measurement. Specimens for mechanical measurement had a dimension of 1.5 × 4.00 × 25.4 mm with a deviation of thickness of 0.01 mm. Tensile testing was performed at ambient temperature according to ASTM procedure D3039 using a United Testing System. The strain rate was 0.51 mm/min. The maximum failure strengths and Young's moduli were obtained from the stress–strain curves.

Results and Discussion

The exfoliation of the clay tactoids in a polymer matrix requires a driving force to overcome the attractive electric force between the negative charged silicate layers and the gallery cations. One way to achieve this effect is to use the energy of intergallery self-polymerization reaction as reported in the previous studies of the self-polymerization of Epon-828 in an acidic montmorillonite.[25–27] However, as we learned from these earlier studies, the intergallery polymerization rate should not be much larger than the extra gallery polymerization rate, because this can lead to phase segregation of the polymer and the formation of nonprocessable powders. In the present study we have found that intergallery polymerization and clay layer exfoliation can be regulated in part by selecting hydrophobic alkylammonium exchanged cations that are sufficiently acidic to catalyze the polymerization process. Before intragallery polymerization can be initiated, however, the galleries must be preintercalated by epoxy monomer. Thus, we consider first the factors influencing the intercalation of alkylammonium clays by epoxy resin.

As shown by the data in Table 1, the chain length of the alkylammonium ion greatly effects the extent of clay expansion upon epoxide intercalation. Basal spacings for a series of epoxy-solvated $CH_3(CH_2)_{n-1}NH_3^+$–montmorillonites with n = 4, 8, 10, 12, 16, and 18 increase in proportion to the chain length of the onium ion. Assuming that the gallery cations upon epoxy solvation reorient from their initial monolayer, bilayer, or paraffin-like orientation[32] to a vertical orientation relative in the clay basal surfaces, we expect the basal spacings (Å) to follow the relationship $d_{001} = 1.27(n-1) + d_A + r_M$, where $(n-1)$ is the number of methylene groups in the onium ion chain, d_A is the basal spacing for NH_4^-–montmorillonite (12.8 Å), r_M is the van der Waals radius of the methyl end group (3.0 Å), and 1.27 Å is the contribution due to the $-CH_2-$ chain segments when the chain adopts an all-trans configuration. This latter assumption is an approximation since recent infrared studies by Giannelis and co-workers have shown that gauche conformation of the chains can be abundent.[33]

For $CH_3(CH_2)_3NH_3^+$–montmorillonite, the observed basal spacing is somewhat smaller than the value calculated for a vertical onium ion orientation, suggesting that this shorter chain ion may adopt an inclined orientation in epoxy-solvated gallery. For alkylammonium ions with $n \geq 8$, however, the basal spacing is very near the calculated value for a vertical or near-vertical onium ion orientation. By subtracting the van der Waals thickness of the clay layer (9.6 Å) from the basal spacings of the epoxy-solvated $CH_3(CH_2)_{n-1}NH_3^+$ montmorillonites in Table 1, we find that the gallery height increases from 6.9 Å for n = 4 to 17.4–27.1 Å for onium ions with n in the range 8–18. On the basis of computer modeling the van der Waals dimensions of the epoxy monomer are 14.6 × 4.4 × 3.5 Å. Therefore, the epoxy can intercalate only a monolayer into $CH_3(CH_2)_3NH_3^+$–montmorillonite, but for intercalated onium ions with $n \geq 8$ multiple layers of epoxy monomers can be accommodated in the galleries.

The addition of the curing agent mPDA to epoxide–clay mixtures at room temperature resulted in little or no change in the clay basal spacings. However, upon initiating cross-linking at elevated temperatures,[31] significant changes in clay basal spacings were observed.

XRD patterns for mPDA cross-linked epoxy–clay composites containing 5 wt % $CH_3(CH_2)_{15}NH_3^+$–montmorillonite cured under different thermal conditions are shown in Figure 2. The composites cured slowly at 75 °C for 4 h or rapidly at 140 °C for 4 h exhibit broad Bragg diffraction peaks at 32 and 34 Å, respectively. In contrast, the same compositions cured at intermediate rates by a two-stage curing process (first at 75 °C for 2 h and then at 125 °C for 2 h) or at 125 °C for 4 h do not exhibit diffraction peaks. The absence of Bragg scattering indicates that the clay tactoids have been completely exfoliated (delaminated) by the polymerization process into individual, 10-Å-thick layers to form a nanocomposite. The change in structure that occurs upon converting $CH_3(CH_2)_{15}NH_3^-$–montmorillonite into the epoxide solvated form and finally into a cured polymer-exfoliated clay nanocomposite is illustrated in Figure 3.

---

(32) Lagaly, G.; Beneke, K.; Weiss, A. *Am. Miner.* **1975**, *60*, 642.

(33) Vaia, R. A.; Teukolsky, R. K.; Giannelis, E. P. *Chem. Mater.* **1994**, *6*, 1017.

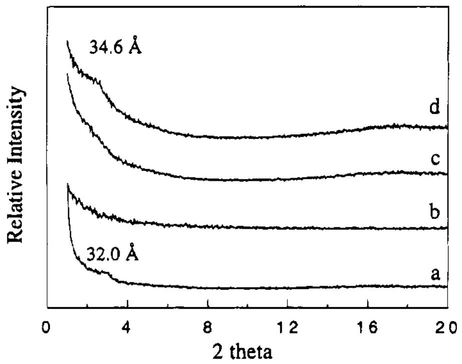

Figure 2. X-ray diffraction patterns of amine-cured epoxy–clay composites containing 5 wt % $CH_3(CH_2)_{15}NH_3^+$–montmorillonite following different curing treatments: (a) 4 h at 75 °C, (b) 2 h at 75 °C followed by 2 h at 125 °C, (c) 4 h at 100 °C, and (d) 4 h at 140 °C.

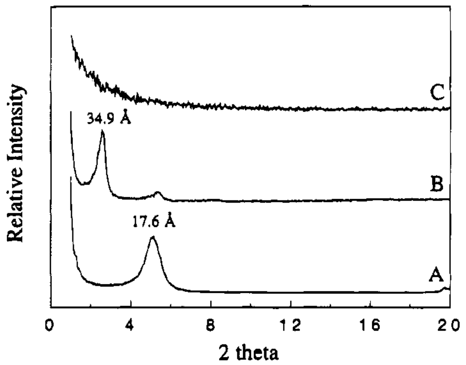

Figure 3. X-ray diffraction patterns of $CH_3(CH_2)_{15}NH_3^+$–montmorillonite in different physical states: (A) pristine clay, (B) 5 wt % clay in Epon-828 suspension, and (C) exfoliated clay (5 wt %) in a mPDA-cured epoxy nanocomposite.

Because the amount of resin that can be loaded into the galleries of an organo clay is dependent on the chain length of the onium cation, the degree of organoclay exfoliation in a mPDA–epoxy matrix also will depend on the gallery cations. XRD diffraction patterns for cured epoxy–clay composites containing 5 wt % of various alkylammonium exchanged forms of montmorillonites are shown in Figure 4. The results for NH_4^+– and Na^+–montmorillonite are included for comparison. Composites formed with $CH_3(CH_2)_7NH_3^+$–, $CH_3(CH_2)_{11}NH_3^+$–, and $CH_3(CH_2)_{15}NH_3^+$–montmorillonite exhibit no Bragg scattering, indicating that the clay has been exfoliated into 10-Å-thick layers with no regular repeat distance between the layers. That is, the clay layer separation is large (>80 Å) and highly disordered. It is noteworthy that $CH_3(CH_2)_3NH_3^+$–montmorillonite with an initial d_{001} of 13.5 Å characteristic of a monolayer of onium ion, gives rise to a diffraction peak at 16.6 Å under mPDA-cured conditions, indicating that a polymer monolayer is formed in the clay gallery. This latter material is an intercalated nanocomposite. No layer exfoliation or intercalation was observed for NH_4^+ and Na^+ exchanged montmorillonite. Thus, montmorillonites intercalated by alkylammonium cations with chain length larger than eight carbon atoms yield nanocomposites, whereas the clays interlayered by shorter alkylammonium cations and simple inorganic cations tend to afford intercalated nanocomposite architecture and conventional phase-segregated composites, respectively.

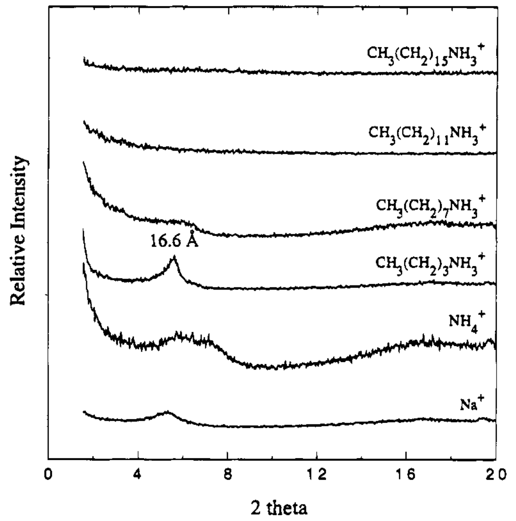

Figure 4. X-ray patterns of epoxy–clay composite materials formed by the polymerization of a DGEBA resin, Epon-828, with a stoichiometric amount of mPDA as the curing agent in the presence of various cation exchanged forms of montmorillonite. The exchange ions are identified for each diffraction pattern.

The dependence of nanocomposite formation on onium ion chain length can be explained by the following general reaction mechanism. Swelling of clay by the epoxy monomers controls the initial accessibility of the galleries for polymer formation. Long-chain alkylammonium exchanged montmorillonites solvated by the epoxy provide a hydrophobic environment for mPDA to migrate into the clay interlayer region. Under appropriate curing conditions more epoxy and mPDA penetrate the gallery space and intragallery polymerization can occur at a rate that is comparable to extragallery polymerization. Consequently, the galleries continue to expand as the degree of polymerization increases and a monolithic exfoliated nanocomposite is formed. However, if the curing temperature is too low and the rates of epoxy and mPDA intercalation is too slow, then extragallery polymerization will be faster than intragallery polymerization and intercalated nanocomposites will form. Intercalated nanocomposites also will form if the extragallery curing is favored by curing at high temperature. Thus, it is important to select curing conditions that balance the intra- and extragallery polymerization rates. Short alkylammonium exchange ions on the gallery surfaces make intragallery diffusion more restrictive, and it becomes more difficult to achieve the curing conditions needed to balance the rates of intra- and extragallery polymerization. Consequently, intercalated clay nanocomposite structures tend to be formed. Inorganic exchanged forms of montmorillonite are hydrophilic and not readily swelled by epoxy monomers, making intragallery polymerization impossible. Therefore, conventional phase-separated composites are formed for Na^+– and NH_4^+–montmorillonites.

Owing to the spatially restricted nature of the gallery environment, one might not expect the intragallery polymerization rate to be competitive with the extragallery rate under any curing conditions. However, the alkylammonium ions that favor clay layer exfoliation are acidic and can catalyze the epoxy–amine polymer-

Table 2. Basal Spacings for Air-Dried and Epoxy-Solvated $CH_3(CH_2)_{15}NH_3^+$-Exchanged Clays

clay	CEC[a] (mequiv/100 g)	air-dried d_{001}, Å	cation orientation[b]	epoxy solvated, Å
hectorite	67	18.0	bilayer	35.3
montmorillonite	90	17.5	bilayer	34.1
fluorohectorite	122	28.0	paraffin	33.7
vermiculite	200	28.6	paraffin	34.9

[a] Cation exchange capacity, mequiv/100 g of clay. [b] Orientation of the alkylammonium ion under air-dried conditions.

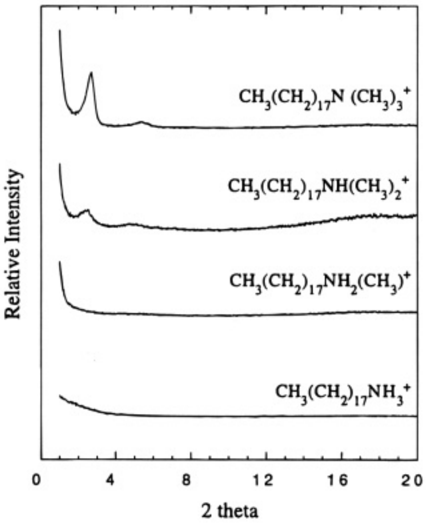

Figure 5. X-ray powder diffraction patterns of amine-cured epoxy–clay nanocomposites formed from montmorillonite clays (5 wt %) containing primary, secondary, tertiary, and quaternary onium ions with a *n*-C18 chain lengths.

ization reaction.[34–36] The importance of intragallery catalysis is illustrated by the decrease in layer exfoliation with decreasing Bronsted acidity of the exchange ion in the order $CH_3(CH_2)_{17}NH_3^+ > CH_3(CH_2)_{17}N(CH_3)H_2^+ > CH_3(CH_2)_{17}N(CH_3)_2H^+ > CH_3(CH_2)_{17}N(CH)_3^+$. For these onium ions, the initial swelling of the clay by the epoxy monomer is essentially constant (d_{001} = 36.2–36.9 Å) simply because the epoxy intercalation is determined by the C_{18} chain length of the gallery cations. But the X-ray diffraction results for the amine-cured epoxy–clay composites, as shown in Figure 5, indicate the clays with primary and secondary onium ions form exfoliated nanocomposites, whereas the clays with tertiary and quaternary onium ions retain the clay tactoid structure typical of intercalated nanocomposites.

To verify the importance of onium ion–epoxy solvation in preloading the clay galleries, we have investigated the effect of clay layer charge on swelling. Hectorite, montmorillonite, fluorohectorite, and vermiculite represent a series of 2:1 clays of increasing layer charge density. Basal spacings for the $CH_3(CH_2)_{15}NH_3^+$ exchanged form of these clays solvated by the epoxy resin monomers are listed in Table 2. It is especially significant that the basal spacings for the epoxy-intercalated clays are essentially independent of the layer charge density of the starting clay. These results again show that the initial swelling of the clay is controlled by the sorptive interactions between vertically oriented gallery organocations and the epoxy resin.

The model illustrated in Figure 6 summarizes the overall mechanism for formation of epoxy polymer–clay nanocomposites. Upon solvation of the organoclay by the epoxide monomers, the gallery cations reorient from their initial monolayer, lateral bilayer, or inclined paraffin structure to a *perpendicular* orientation with epoxy molecules inserted between the onium ions. The basal spacings suggest that an all trans configuration is adopted by the alkylammonium chain. A related reorientation of alkyl ammonium ions has been observed previously for ϵ-caprolactam intercalated clay intermediates formed in the synthesis of Nylon-6-exfoliated clay nanocomposites.[23] Thus, the ability of the onium ion chains to reorient into a vertical position in order to optimize solvation interactions with the monomer may be a general prerequisite for preloading the clay galleries with sufficient monomer to achieve layer exfoliation upon intragallery polymerization.

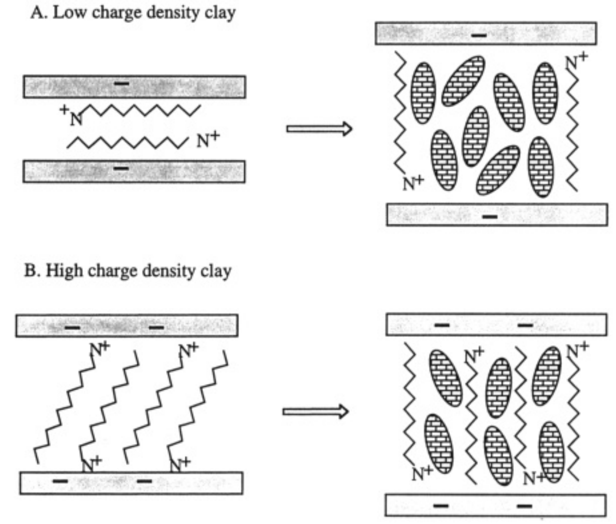

Figure 6. Proposed model for the swelling of alkylammonium exchanged clay by Epon-828: (A) low charge density clay with a lateral bilayer structure and (B) high charge density clay with a paraffin structure. Regardless of the initial charge density of the clay and orientation of the gallery alkylammonium, the gallery height is determined by the vertical orientation of the organocations in the solvated intercalates. Cross-hatched ellipses represent the intercalated resin molecules.

The amount of epoxy monomer that can be preloaded into organoclay galleries will depend on the clay layer charge density and the length of the organic cation. For clays with a high layer charge density, a large number of gallery onium ions are needed to balance the layer charge. Therefore, because of the increasing population density of gallery onium ions, fewer epoxide monomers will be accommodated inside the clay galleries as the layer charge density is increased. Clays preintercalated with different amounts of the epoxy monomers are expected to perform differently with regard to exfoliation and nanocomposite formation.

Accordingly, composites containing primary alkylammonium exchanged form of hectorite, montmorillonite, fluorohectorite, and vermiculite have been prepared in order to examine the effect of charge density

---

(34) Kamon, T.; Furakaw, H. *Adv. Polym. Sci.* **1986**, *80*, 177.
(35) Barton, J. M. *Adv. Polym. Sci.* **1985**, *72*, 120.
(36) May, C. A., Ed. *Epoxy Resins*, 2nd ed.; Marcel Dekker: New York, 1988.

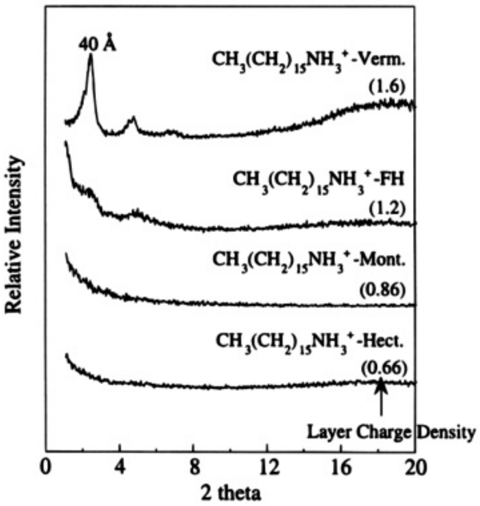

Figure 7. X-ray diffraction patterns of amine-cured epoxy–clay composite hybrids formed by the polymerization of a DGEBA resin, Epon-828, with stoichiometric amounts mPDA as a curing agent in the presence of various clays with $CH_3(CH_2)_{17}NH_3^+$ as exchanged cations for different layer charge density clays. Layer charge density values (mequiv/g) are given in parentheses.

on nanocomposite formation. X-ray powder diffraction patterns of the amine-cured epoxy–clay composites formed with 5 wt % loading of $CH_3(CH_2)_{15}NH_3^+$–hectorite, –montmorillonite, –fluorohectorite, and –vermiculite are shown in Figure 7. For hectorite and montmorillonite, no d_{001} diffraction peaks are observed, indicating that these clays are exfoliated in the epoxy matrix. The X-ray diffraction pattern of the composite with fluorohectorite shows board diffraction peaks, corresponding to basal spacing of 37 Å. This indicates that for a significant fraction of the clay the layer separation of fluorohectorite is increased only slightly from the value of 34 Å for the uncured epoxy solvated intercalate. For vermiculite, there is a well-expressed d_{001} diffraction, corresponding a very well defined basal spacing of 36 Å. These results suggest that clays with high layer charge density and a correspondingly high population density of onium ions limit intragallery diffusion of epoxy and amine and tend to form intercalated nanocomposites rather than exfoliated nanocomposites.

Intercalated and exfoliated nanocomposite formation also may be distinguished on the bases of transmission electron microscopy. As shown by the TEM image in Figure 8 for the composite containing 5 wt % of exfoliated $CH_3(CH_2)_{15}NH_3^+$–montmorillonite the separation between the highly dispersed plates is irregular and in the range 60–200 Å. TEM images of the analogous composites formed from hectorite, fluorohectorite, and vermiculite are provided in Figure 9. The dispersion of the clay platelets in the exfoliated hectorite composite is very similar to that of montmorillonite (Figure 8) but with smaller silicate plates. For the fluorohectorite, many of the silicate layers retain an ordered tactoid structure with a basal spacing around 40 Å, consistent with the X-ray diffraction results, other arrays of layers are exfoliated with interlayer distances in the range 50–140 Å. Thus, the fluorohectorite composite may be considered a partially intercalated nanocomposite. On the other hand vermiculite forms mainly an intercalated nanocomposite as most of the clay layers exhibit very well ordered stacking with a basal spacing of about 40 Å, consistent with the X-ray diffraction result.

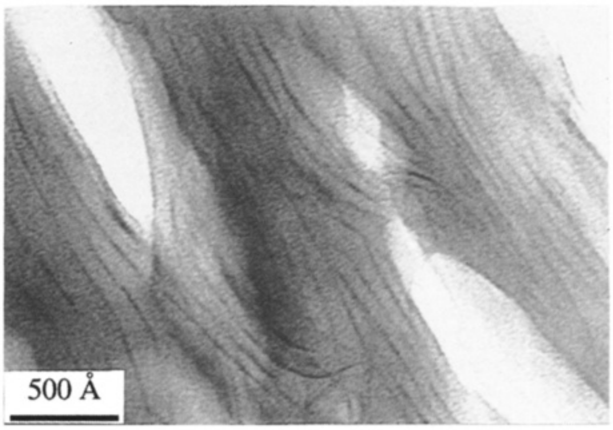

Figure 8. TEM of an amine-cured epoxy-exfoliated clay nanocomposite structure formed with $CH_3(CH_2)_{15}NH_3^+$–montmorillonite (5 wt %).

On the basis of the above XRD and TEM results, we may conclude that clays with a low-to-moderate layer charge density, such as hectorite and montmorillonite, are very good candidates for formation of epoxy-exfoliated clay nanocomposites. They exhibit excellent swelling properties toward organic monomers. A low population density of alkylammonium ions in the gallery provides more intergallery space to accommodate mPDA and epoxy monomers and to initiate formation of an intragallery polymer network. Also, the limited polymer network is sufficiently mobile to facilitate further migration of the monomers into the gallery for further exfoliation. For vermiculite, too little epoxy resin is initially present inside the galleries, the onium ion–polymer network is too rigid, and the resulting composite is an intercalated nanocomposite. Fluorohectorite exhibits better exfoliation than vermiculite, because of its lower layer charge density, but much of the clay remain intercalated upon polymer curing.

To access the benefit of clay exfoliation in the epoxy matrix, the tensile strengths and moduli for the amine-cured epoxy–clay nanocomposites have been determined for loadings in the range 1–2 wt %. For the pristine amine-cured epoxy matrix, the tensile strength is 90 MPa and the tensile modulus is 1.1 GPa. Comparing the mechanical properties of the exfoliated and intercalated nanocomposite in Figure 10 and Table 3, we find that the exfoliated nanocomposites show improved performance, in the modulus but not in the tensile strength, relative to the pristine polymer. As expected, the benefit derived for this brittle epoxy matrix ($T_g \sim 150$ °C) is not as great as we observed previously for a rubbery epoxy matrix ($T_g \sim -40$ °C).[12,29] Nevertheless, consistent with our earlier findings, exfoliated clay composites are favored over intercalated analogues for improving the mechanical performance of a polymer.

Conclusions

Alkylammonium exchanged clays are excellent materials for the synthesis of hybrid epoxy–inorganic nanocomposites. Long-chain alkylammonium ions allow epoxy monomers to be accommodated in the gallery by adopting a vertical orientation that optimizes solvation interactions with the alkyl chains. Two types of amine-

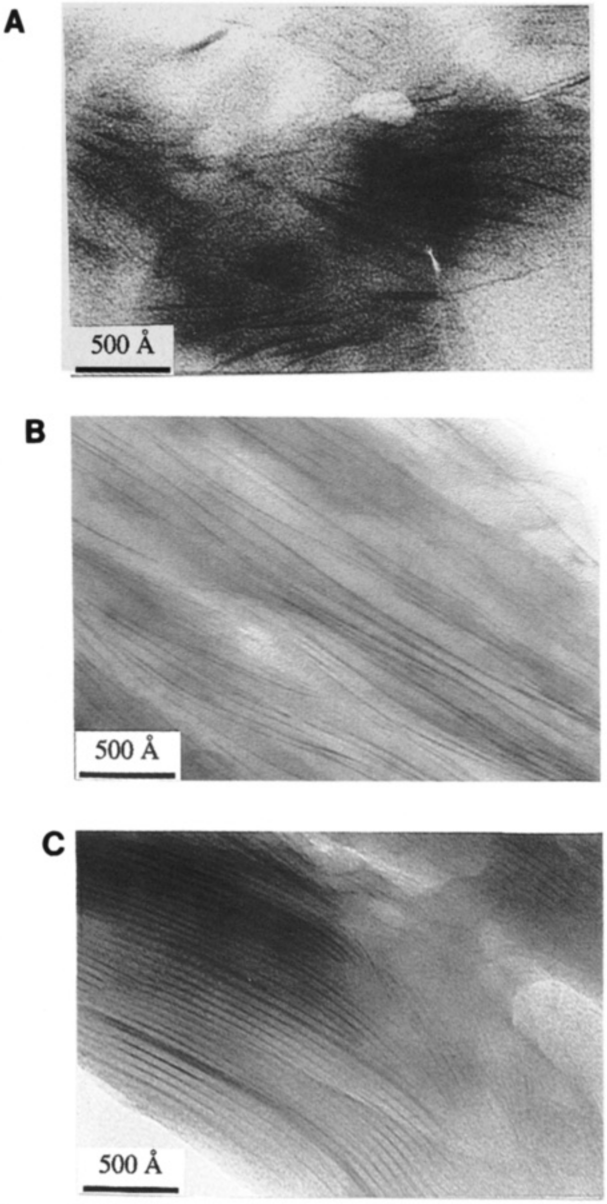

Figure 9. TEM images of amine-cured epoxy–clay nanocomposite with a clay content of 5 wt %. Epoxy exfoliated clay nanocomposite architecture obtained with (A) $CH_3(CH_2)_{15}NH_3^+$–hectorite. Intercalated epoxy–clay nanocomposite structures obtained with (B) $CH_3(CH_2)_{15}NH_3^+$–fluorohectorite and (C) $CH_3(CH_2)_{15}NH_3^+$–vermiculite.

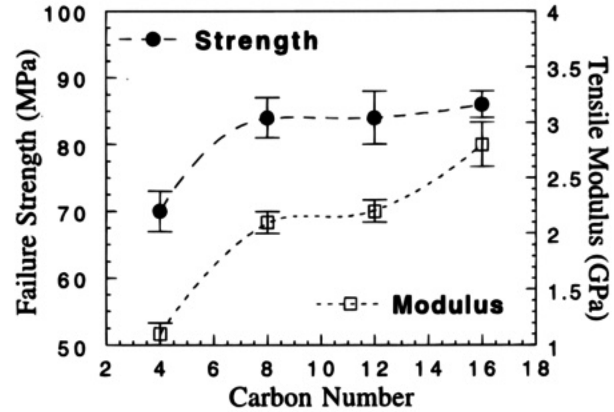

Figure 10. Dependence of tensile strength and modulus of amine-cured epoxy–clay nanocomposites on onium ion carbon number at clay loadings of 2 wt %.

Table 3. Mechanical Properties of Epoxy–Clay Nanocomposites Containing 1.0 wt % $CH_3(CH_2)_{15}NH_3^+$-Exchanged Clays

clay	failure strength (MPa)	tensile modulus (GPa)
none	90 ± 3	1.10 + 0.03
hectorite	94 ± 2	1.65 ± 0.03
montmorillonite	92 ± 5	1.49 ± 0.03
fluorohectorite	73 ± 3	1.55 ± 0.06

cured epoxy–clay hybrid nanocomposites, namely, intercalated and exfoliated clay composites, can be prepared by tuning the curing rates inside and outside clay gallery regions. Onium ions with Bronsted acidity catalyze intragallery polymerization at rates that are competitive with extragallery polymerization rates. Thus, the acidic onium ion clays facilitate clay tactoid exfoliation and the formation of monolithic exfoliated clay nanocomposite architecture. Aprotic quaternary ammonium ions tend to form intercalated clay nanocomposites, which are less effective than exfoliated analogues in enhancing the mechanical properties of the polymer. The layer charge density of the pristine clays mediates the amount of monomer that can be preintercalated in the intergallery region. Consequently, clays with low-to-intermediate charge densities (hectorite and montmorillonite) are best suited for the formation of exfoliated clay nanocomposites.

Acknowledgment. The partial support of this research by the Michigan State University Center for Fundamental Materials Research and the National Science foundation (CRG Grant CHE-9224102) is gratefully acknowledged.

CM950226E